Stability of the Active Flux Method in the Framework of Summation-by-Parts Operators

Wasilij Barsukow[1], Christian Klingenberg[2], Lisa Lechner[2],
Jan Nordström[3,4], Sigrun Ortleb[5], and Hendrik Ranocha[6]

[1]Corresponding author, wasilij.barsukow@math.u-bordeaux.fr, Institut de Mathématiques de Bordeaux (IMB), CNRS UMR 5251, 351 Cours de la Libération, 33405 Talence, France
[2]University of Würzburg, Institute of Mathematics, Emil-Fischer-Straße 40, 97074 Würzburg, Germany

[3]Department of Mathematics, Linköping University, SE-581 83 Linköping, Sweden

[4]Department of Mathematics and Applied Mathematics, University of Johannesburg, Auckland Park 2006, Johannesburg, South Africa

[5]University of Kassel, Institute of Mathematics, Untere Königsstraße 86, 34117 Kassel, Germany

[6]Johannes Gutenberg University Mainz, Institute of Mathematics, Staudingerweg 9, 55128 Mainz, Germany

February 18, 2026

The Active Flux method is a numerical method for conservation laws using a combination of cell averages and point values as independent degrees of freedom, based on ideas from finite volumes and finite differences. This unusual mix has been shown to work well in many situations. We expand the theoretical justifications of the Active Flux method by analyzing it from the point of view of summation-by-parts (SBP) operators, which are routinely used to analyze finite difference, finite volume, and finite element schemes. We investigate in what type of setting the Active Flux method can be formulated using classical or degenerate SBP operators, yielding a first and novel approach for showing the energy stability of the Active Flux method. We present the analysis for the one-dimensional scalar linear advection equation with periodic boundary conditions on a uniform grid.

Key words. Active Flux method, summation-by-parts operators, conservation laws, finite difference methods, finite volume methods
AMS subject classification. 65M06, 65M20, 65M70

1. Introduction

The Active Flux schemes are a class of methods introduced to solve systems of hyperbolic conservation laws (see [18–20]), an extension of Scheme V from [34]. They combine two types of degrees of freedom: cell averages and shared point values at the cell interfaces. The Active Flux method uses a globally continuous approximation, which is conceptually different to other finite volume

methods. Yet, the conservative updates of the cell averages resemble a finite volume method and are given by the fluxes through the boundary of the cell. The Active Flux method approximates these fluxes by quadratures directly using the point values. This is in contrast to many finite volume schemes that use Riemann solvers to define the fluxes.

Two ways how the point values can be updated in time have emerged. Initially (e.g., in [20, 34]), it was proposed to use a short-time (approximate) solution of the initial-value problem (IVP) of the conservation law. Such an approach is appropriate for many equations (see [7, 18] for scalar conservation laws and for hyperbolic systems of conservation laws in one spatial dimension) and the resulting method is a one-stage method. The solution of the IVP naturally includes upwinding which is helpful for stability upon explicit integration in time. Since it is quite challenging to find short-time (approximate) third-order accurate solutions for multi-dimensional systems of conservation laws, it was proposed in [5, 6] to complement a semi-discrete version of the cell average update with an ordinary differential equation (ODE) for the point value and to integrate both in time using a standard Runge-Kutta method [1–3].

The aim of this paper is to provide the first energy stability analysis of a semi-discrete Active Flux scheme using the framework of summation-by-parts (SBP) operators. The Active Flux method distinguishes itself through its low dissipation and dispersion property ([54]). Especially in multiple space dimensions it has structure preserving properties that are unrivaled by comparable schemes: it maintains vortical structures even on coarse cells, it preserves stationary states, it is asymptotic preserving without changing the scheme ([9]). SBP operators are used to mimic the integration-by-parts rule on the discrete level. Energy stability of the resulting numerical schemes is then analyzed using matrix properties of the involved SBP operators. For a good grasp on this concept, we recommend the review papers [21, 62]. By the SBP property, the continuous energy stability analysis for a given partial differential equation can be transferred to a (semi-)discrete energy stability analysis of the numerical scheme. Thus, energy stability may be ensured for a variety of PDEs when augmented with appropriate numerical boundary conditions, e.g., via simultaneous approximation terms (SATs) first introduced in [13].

Discrete derivative operators with an SBP property have originally been considered and developed in the context of finite difference schemes for hyperbolic and parabolic problems, see, e.g., [13, 33, 41, 42, 56], with the aim to construct high-order accurate, conservative and stable numerical methods for hyperbolic and parabolic PDEs including variable coefficient equations and nonlinear hyperbolic conservation laws. More recent investigations also focus on SBP operators within various popular classes of numerical schemes, e.g., finite volume schemes [39, 40], continuous finite element [4, 29, 30], discontinous Galerkin (DG) schemes [12, 14, 22, 43], flux reconstruction (FR) schemes [31, 51, 65], as well as meshless methods [28]. In addition, SBP operators based on general function spaces have been constructed in [23–26].

The classical SBP framework considers central difference operators, whereas the Active Flux method uses upwinding. The concept of upwinding was introduced directly in the SBP framework in [37] as a special case of dual-pair derivative operators [17]. Upwind SBP operators can be interpreted as classical central SBP operators plus artificial dissipation [38, 60] resulting in one-sided difference stencils. Furthermore, they arise when coupling multiple SBP operators on subdomains of the complete spatial domain either by interface SATs [49] or by numerical fluxes [44]. The discovery of central and upwind SBP properties in various high-order schemes suggests that some form of SBP property is an essential feature in any type of provably energy stable, high-order accurate numerical method.

This work investigates the SBP properties of the semi-discrete Active Flux method for linear advection with periodic boundary conditions and analyzes its energy stability. To the best of our knowledge, this is the first attempt to prove energy stability for this method in the SBP framework. The definition of an SBP operator includes a mass matrix (or norm matrix) in addition to the discrete derivative operator. This mass matrix is used in the discrete integration-by-parts rule and in the definition of the discrete energy norm under which energy stability is studied. Given a discrete derivative operator, first, a suitable mass matrix needs to be found for the SBP property

to hold. In this work, we investigate the potential existence and form of such a mass matrix for the Active Flux method in one-dimensional periodic setting. First, we consider the central version of the standard semi-discrete Active Flux method for the linear advection equation with periodic boundary conditions and show that the resulting discrete derivative operator admits a diagonal mass matrix resulting in a periodic diagonal-norm SBP operator. Energy stability of the Active Flux method in this periodic setting then follows in straightforward manner by SBP properties.

Furthermore, we consider the original semi-discrete Active Flux method based on upwinding. For this scheme, a non-diagonal positive semi-definite mass matrix is found such that the pair of Active Flux methods for positive and negative advection coefficients results in a dual-pair of periodic upwind SBP operators. Our analysis shows that a diagonal mass matrix leading to an upwind SBP property of the upwind Active Flux method does not exist. Even though the mass matrix is not positive definite since its kernel contains the multiples of the all-ones vector $\mathbf{1}$, we prove energy stability of the Active Flux method in the SBP framework by an additional study of the solution component in the kernel of the norm matrix.

In addition, nullspace consistency of the Active Flux method is investigated in this work. Nullspace consistency was introduced in [61] and signifies that the nullspace of the continuous derivative operator is correctly transferred to its discrete counterpart and that no spurious modes lie in the discrete kernel. Classical central SBP operators for periodic problems are not nullspace consistent due to their skew-symmetric character and the central Active Flux scheme is no exception. However, periodic upwind SBP operators can be nullspace consistent and we prove nullspace consistency of the original semi-discrete Active Flux method based on upwinding.

This paper is organized as follows. We start by introducing the Active Flux method and defining periodic SBP operators in section 2. Section 3 analyzes the Active Flux method in the SBP framework. First, a central version of the Active Flux method is considered, which fits the more classical central SBP framework. Then, the semi-discrete upwind Active Flux method is analyzed using the insight gained from the analysis of the central scheme. The stability results are summarized in section 4 and verified in section 5 by numerical experiments. Nullspace consistency of the upwind Active Flux difference operators is proven in section 6. In order to increase readability, section A collects some detailed technical aspects employed to study the SBP properties and section B provides a relation to the von Neumann stability concept.

2. General aspects of Active Flux and SBP operators

We begin by introducing the *Active Flux method* for conservation laws, originally proposed in [20, 34]. Even though this method shows its real strength in two and three space dimensions, we restrict ourselves to one space dimension for simplicity and clarity. Consider the scalar conservation law

$$\partial_t u(x,t) + \partial_x f(u(x,t)) = 0 \tag{2.1}$$

on domain $\Omega = [x_{\min}, x_{\max}] \subset \mathbb{R}$ with $u : \Omega \times [0,\infty) \to \mathbb{R}$, $f : \mathbb{R} \to \mathbb{R}$ and periodic boundary conditions. Later, (2.1) will be simplified to the linear constant coefficient advection equation

$$\partial_t u + a\partial_x u = 0. \tag{2.2}$$

Our results hold for general constants $a \in \mathbb{R}$ but as an indicator, we often choose $a = 1$ or $a = -1$.

2.1. The Active Flux method

Consider a computational grid with n cells $[x_{i-\frac{1}{2}}, x_{i+\frac{1}{2}}]$ and cell centers $x_i = \frac{x_{i+\frac{1}{2}} + x_{i-\frac{1}{2}}}{2}$, $i = 0, \dots, n-1$. For simplicity, all cells have the same size $\Delta x := x_{i+\frac{1}{2}} - x_{i-\frac{1}{2}}$. The Active Flux method uses cell averages u_i and point values $u_{i+\frac{1}{2}}$ as degrees of freedom, see Figure 1. The point values are placed at the cell interfaces and shared by adjacent cells.

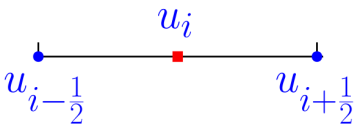

Figure 1: A cell that goes from $x_{i-\frac{1}{2}}$ to $x_{i+\frac{1}{2}}$ is shown: u_i is the cell average of the solution u, whereas $u_{i+\frac{1}{2}}$ and $u_{i-\frac{1}{2}}$ are its point values. With these three pieces of information one can reconstruct a parabola in this cell. Since the point values are shared with neighboring cells, one associates with each cell two degrees of freedom, namely $u_{i-\frac{1}{2}}$ and u_i.

The three pieces of information accessible to each cell (two point values and the cell average) allow for a parabolic reconstruction $u_{\text{recon},i}\colon \left[-\frac{\Delta x}{2}, \frac{\Delta x}{2}\right]$, which fulfills

$$u_{\text{recon},i}\left(\pm\frac{\Delta x}{2}\right) = u_{i\pm\frac{1}{2}}, \qquad \frac{1}{\Delta x}\int_{-\frac{\Delta x}{2}}^{\frac{\Delta x}{2}} u_{\text{recon},i}(x)\,\mathrm{d}x = u_i. \tag{2.3}$$

We find $u_{\text{recon},i} = \frac{6u_i - u_{i+\frac{1}{2}} - u_{i-\frac{1}{2}}}{4} + \frac{u_{i+\frac{1}{2}} - u_{i-\frac{1}{2}}}{\Delta x}x + 3\frac{u_{i+\frac{1}{2}} + u_{i-\frac{1}{2}} - 2u_i}{\Delta x^2}x^2$. The global reconstruction $u_{\text{recon}}(x)\colon \mathbb{R} \to \mathbb{R}$ is piecewise parabolic and continuous:

$$u_{\text{recon}}(x) = u_{\text{recon},j}(x - x_j) \quad \text{if} \quad x \in [x_{j-\frac{1}{2}}, x_{j+\frac{1}{2}}], \quad j \in \mathbb{N}. \tag{2.4}$$

When integrating the conservation law (2.1) over the cell, Gauss' law allows us to couple the cell averages and the point values:

$$\frac{\mathrm{d}}{\mathrm{d}t}u_i + \frac{f(u_{i+\frac{1}{2}}) - f(u_{i-\frac{1}{2}})}{\Delta x} = 0. \tag{2.5}$$

Next, we need to determine the point value updates. In this paper, we restrict ourselves to one *upwind* and one *central* point update.

The semi-discrete upwind point update is given by

$$\frac{\mathrm{d}}{\mathrm{d}t}u_{i+\frac{1}{2}} + f'(u_{i+\frac{1}{2}})(d_x^{\text{upw}}u)_{i+\frac{1}{2}} = 0 \tag{2.6}$$

combined with an upwind finite difference formula $(d_x^{\text{upw}}u)_{i+\frac{1}{2}}$:

$$(d_x^{\text{upw}}u)_{i+\frac{1}{2}} := \begin{cases} \frac{\mathrm{d}}{\mathrm{d}x}u_{\text{recon}}(x^-_{i+\frac{1}{2}}), & f'(u_{i+\frac{1}{2}}) > 0, \\ \frac{\mathrm{d}}{\mathrm{d}x}u_{\text{recon}}(x^+_{i+\frac{1}{2}}), & \text{else}, \end{cases} = \begin{cases} \frac{\mathrm{d}}{\mathrm{d}x}u_{\text{recon},i}\left(\frac{\Delta x}{2}\right), & \text{if} \quad f'(u_{i+\frac{1}{2}}) > 0, \\ \frac{\mathrm{d}}{\mathrm{d}x}u_{\text{recon},i+1}\left(-\frac{\Delta x}{2}\right), & \text{else}. \end{cases} \tag{2.7}$$

By construction, the finite differences are thus exact for parabolae. The discontinuity in the derivative of u_{recon} at $x_{i+\frac{1}{2}}$ allows one to include upwinding. In [6], the scheme (2.5)-(2.7) has been found to be L^2-stable with RK3 up to a CFL number of approximately 0.4 using Fourier analysis.

From now on, we focus on the linear advection equation (2.2). For $a = 1$, we have

$$\frac{\mathrm{d}}{\mathrm{d}t}u_{i+1/2} + \frac{2u_{i-1/2} - 6u_i + 4u_{i+1/2}}{\Delta x} = 0. \tag{2.8}$$

For $a = -1$, we have

$$\frac{\mathrm{d}}{\mathrm{d}t}u_{i+1/2} - \frac{-4u_{i+1/2} + 6u_{i+1} - 2u_{i+3/2}}{\Delta x} = 0. \tag{2.9}$$

More about point updates in the Active Flux method, and convergence analyses confirming experimentally the third order of accuracy can be found in [6] and papers referenced therein. The

semi-discrete Active Flux method can be extended to multiple dimensions and to higher orders of accuracy, see [8].

The point value update employs a *central discretization* will be used in the theoretical analysis below. A central derivative is obtained by taking the average of the two options (2.8) and (2.9)

$$(d_x^{\text{central}} u)_{i+\frac{1}{2}} := \frac{1}{2}\left(\frac{\mathrm{d}}{\mathrm{d}x} u_{\text{recon},i}\left(\frac{\Delta x}{2}\right) + \frac{\mathrm{d}}{\mathrm{d}x} u_{\text{recon},i+1}\left(-\frac{\Delta x}{2}\right)\right), \tag{2.10}$$

which leads to the following update formula

$$\frac{\mathrm{d}}{\mathrm{d}t} u_{i+1/2} + \frac{u_{i-1/2} - 3u_i + 3u_{i+1} - u_{i+3/2}}{\Delta x} = 0. \tag{2.11}$$

Remark 2.1. The Active Flux method described above is conservative, since summing up the cell-averages (2.5) leads to conservation. That the point value updates inserted into this formula may themselves be found using a non-conservative update, does not change this fact. Indeed (2.5) will guarantee by the Lax-Wendroff theorem that if the solution converges, it converges to a weak solution. ◁

2.2. The summation-by-parts approach for showing energy stability

In the following, one-dimensional periodic first-derivative SBP operators are introduced. Consider a semi-discretization of the linear advection equation (2.2) with $a = 1$ supplemented by periodic boundary conditions

$$\frac{\mathrm{d}}{\mathrm{d}t}\boldsymbol{u} + D\boldsymbol{u} = \mathbf{0}, \tag{2.12}$$

where $\boldsymbol{u}$ is the vector of unknowns and D the corresponding difference operator. A SBP operator on the interval $\Omega = [x_{\min}, x_{\max}]$ is associated to a vector $\boldsymbol{x}$ of discrete grid nodes within Ω corresponding to the unknowns. Due to the matrix-vector formulation of SBP schemes, we use the notation $\mathbf{1} = (1, \ldots, 1)^T, \mathbf{0} = (0, \ldots, 0)^T$ for the values of these constant functions on the given grid.

An SBP operator D mimics the continuous integration-by-parts property on Ω

$$\int_{x_{\min}}^{x_{\max}} v u_x \mathrm{d}x + \int_{x_{\min}}^{x_{\max}} v_x u \mathrm{d}x = vu\big|_{x_{\min}}^{x_{\max}} \tag{2.13}$$

on the discrete level. Here, we restrict ourselves to periodic boundary conditions, such that the left-hand side of (2.13) vanishes. Then, the periodic SBP property is given as

$$(\mathbf{v}, D\mathbf{u})_M + (D\mathbf{v}, \mathbf{u})_M = 0, \tag{2.14}$$

where M is the symmetric and positive definite norm matrix of the given SBP operator D with the inner product $(u, v)_M = \mathbf{u}^T M \mathbf{v}$.

Considering (2.2) with $a = 1$ and the periodicity of the problem we find

$$\frac{\mathrm{d}}{\mathrm{d}t}\|u\|^2_{L^2(\Omega)} = 2\int_{x_{\min}}^{x_{\max}} u\partial_t u \mathrm{d}x = -2\int_{x_{\min}}^{x_{\max}} u\partial_x u \mathrm{d}x = -u^2(x_{\max}, t) + u^2(x_{\min}, t) = 0 \tag{2.15}$$

from (2.13). Using the SBP operator D with (2.14), the corresponding semi-discrete operation yields

$$\frac{\mathrm{d}}{\mathrm{d}t}\|\boldsymbol{u}\|^2_M = 2\boldsymbol{u}^T M \frac{\mathrm{d}}{\mathrm{d}t}\boldsymbol{u} = -2\boldsymbol{u}^T M D\boldsymbol{u} = -\boldsymbol{u}^T M D\boldsymbol{u} + \boldsymbol{u}^T D^T M \boldsymbol{u} = 0, \tag{2.16}$$

and energy stability is ensured. A periodic SBP operator approximating ∂_x is defined as follows:

Definition 2.2. A *periodic SBP operator* on the interval $[x_{\min}, x_{\max}]$ consists of a grid $\boldsymbol{x}$, a consistent derivative matrix D (with $D\mathbf{1} = \mathbf{0}$), and a symmetric and positive definite mass matrix M (also denoted as norm matrix) such that the periodic SBP property

$$MD + D^T M = 0 \tag{2.17}$$

holds. Since $\int_{x_{\min}}^{x_{\max}} \mathrm{d}x = x_{\max} - x_{\min}$, M is scaled such that $\mathbf{1}^T M \mathbf{1} = x_{\max} - x_{\min}$. We call this SBP operator a *diagonal-norm* SBP operator if M is diagonal. ◁

Remark 2.3. As seen from Definition 2.2, the periodic SBP property implies skew-symmetry of D with respect to M. ◁

A classical first-derivative SBP operator D results from central differences and fulfills (2.17) in the periodic case, where the norm matrix M assumes a role similar to quadrature rules in finite element discretizations. Upwind SBP operators are a special case of dual-pair operators. For periodic boundary conditions, dual-pair upwind SBP operators D_+, D_- discretizing the first derivative fulfill a similar property: $MD_+ + (D_-)^T M = 0$. However, each of the operators D_+ and D_- regarded separately is based on upwind differencing which leads to a built-in artificial dissipation when combined with flux splitting [36, 53, 55]. This approach stabilizes linear problems while retaining the stability properties associated with SBP schemes. Here, we use the following definition:

Definition 2.4. A *periodic upwind SBP operator* on the interval $[x_{\min}, x_{\max}]$ consists of a grid $\boldsymbol{x}$, a pair of consistent derivative matrices D_- and D_+, and a symmetric and positive definite mass matrix M such that the periodic upwind SBP properties

$$MD_+ + D_-^T M = 0, \qquad M(D_+ - D_-) \text{ is negative semidefinite} \tag{2.18}$$

hold. Again, M is scaled to fulfill $\mathbf{1}^T M \mathbf{1} = x_{\max} - x_{\min}$. If M is diagonal, we speak of a *diagonal-norm* upwind SBP operator. ◁

Using periodic upwind SBP operators, a semi-discretization of the linear advection equation (2.2) with $a = 1$ is

$$\frac{\mathrm{d}}{\mathrm{d}t}\boldsymbol{u} + D_-\boldsymbol{u} = \mathbf{0}. \tag{2.19}$$

This method is stable since

$$\frac{\mathrm{d}}{\mathrm{d}t}\|\boldsymbol{u}\|_M^2 = 2\boldsymbol{u}^T M \frac{\mathrm{d}}{\mathrm{d}t}\boldsymbol{u} = -2\boldsymbol{u}^T M D_-\boldsymbol{u} = -\boldsymbol{u}^T M D_-\boldsymbol{u} + \boldsymbol{u}^T D_+^T M \boldsymbol{u} = \boldsymbol{u}^T M(D_+ - D_-)\boldsymbol{u} \le 0. \tag{2.20}$$

Energy stability of the scheme $\frac{\mathrm{d}}{\mathrm{d}t}\boldsymbol{u} - D_+\boldsymbol{u} = \mathbf{0}$ for $a = -1$ is shown similarly.

3. Matrix analysis of the Active Flux method

The following section is dedicated to the analysis of the semi-discrete Active Flux method in the framework of SBP operators. The difficult part consists in finding a suitable mass matrix M whereas the discrete derivative operator D corresponding to the Active Flux method is given. For this purpose, the Active Flux scheme (2.5) and the point update (2.6) for the linear scalar advection equation (2.2) must be rewritten in matrix-vector form. Since periodic boundary conditions are considered, we identify $u_{n-\frac{1}{2}} := u_{-\frac{1}{2}}$. In order to prove SBP properties, we will start with a central version of the Active Flux method since its SBP properties are easier to detect. Afterwards, in the subsequent section, we will turn to the standard upwind version of the Active Flux method.

3.1. Central Active Flux discretization

As motivated before, we aim at formulating the central version of the semi-discrete Active Flux method (given by (2.5) and (2.10)) within the framework of SBP operators which immediately yields stability. The first step to reach this goal consists in establishing a matrix-vector formulation.

We begin by recalling that for the cell averages, the semi-discrete Active Flux method yields the update

$$\frac{\mathrm{d}}{\mathrm{d}t}u_i + \frac{u_{i+1/2} - u_{i-1/2}}{\Delta x} = 0\,. \tag{3.1}$$

We also recall that the point values are updated using a central discretization according to (2.10), which yields

$$\frac{\mathrm{d}}{\mathrm{d}t}u_{i+1/2} + \frac{u_{i-1/2} - 3u_i + 3u_{i+1} - u_{i+3/2}}{\Delta x} = 0. \tag{3.2}$$

Collecting the cell averages u_i and the point values $u_{i+1/2}$ in a single vector $\boldsymbol{u} \in \mathbb{R}^{2n}$, we can write the semi-discrete system in matrix-vector form as

$$\frac{\mathrm{d}}{\mathrm{d}t}\underbrace{\begin{pmatrix} \vdots \\ \hline u_{i-1} \\ \hline u_{i-1/2} \\ \hline u_i \\ \hline u_{i+1/2} \\ \hline u_{i+1} \\ \hline \vdots \end{pmatrix}}_{=:\boldsymbol{u}} + \frac{1}{\Delta x}\underbrace{\left(\begin{array}{ccc|cc|ccc} \ddots & & & & & & & \\ \hline -1 & 0 & 1 & & & & & \\ 1 & -3 & 0 & 3 & -1 & & & \\ \hline & & -1 & 0 & 1 & & & \\ & & 1 & -3 & 0 & 3 & -1 & \\ \hline & & & & -1 & 0 & 1 & \\ & & & & & & \ddots & \end{array}\right)}_{=:D}\boldsymbol{u} = \boldsymbol{0} \tag{3.3}$$

and directly obtain the discrete derivative operator D. Here and below, we add guiding lines to the matrices to make it easier to see which entries belong to point values and cell averages.

We observe that D is skew-symmetric with respect to the diagonal mass matrix

$$M = \frac{\Delta x}{4}\begin{pmatrix} \ddots & & & & & \\ & 3 & & & & \\ & & 1 & & & \\ & & & 3 & & \\ & & & & 1 & \\ & & & & & 3 \\ & & & & & & \ddots \end{pmatrix} \tag{3.4}$$

since

$$MD = -D^T M. \tag{3.5}$$

Therefore, since M is diagonal with positive entries, the discretization of ∂_x via the Active Flux method yields a periodic SBP operator according to Definition 2.2. Hence, we have proved the following theorem.

Theorem 3.1. *The central version* (2.10) *of the semi-discrete Active Flux method can be formulated using SBP operators with derivative matrix D* (3.3) *and diagonal norm/mass matrix M* (3.4)*, satisfying $\mathbf{1}^T M \mathbf{1} = x_{\max} - x_{\min}$.*

Remark 3.2. The diagonal mass matrix M in (3.4) can be interpreted as a chained trapezoidal rule in each cell. Using the transformation of the cell averages $u_i = \frac{1}{6}u_{i-\frac{1}{2}} + \frac{2}{3}u_{i,p} + \frac{1}{6}u_{i+\frac{1}{2}}$ to the cell midpoints $u_{i,p}$ derived from the reconstruction $u_{\mathrm{recon},i}$ and inserting this for the terms $\frac{3}{4}u_i$ shows

$$\mathbf{1}^T M\boldsymbol{u} = \Delta x\left(\cdots + \frac{1}{4}u_{i-\frac{1}{2}} + \left(\frac{1}{8}u_{i-\frac{1}{2}} + \frac{1}{2}u_{i,p} + \frac{1}{8}u_{i+\frac{1}{2}}\right) + \frac{1}{4}u_{i+1/2} + \left(\frac{1}{8}u_{i+\frac{1}{2}} + \frac{1}{2}u_{i+1,p} + \frac{1}{8}u_{i+\frac{3}{2}}\right) + \dots\right).$$

Summing up the point values at cell interfaces and midpoints, we obtain the two variants

$$\mathbf{1}^T M\boldsymbol{u} = \frac{\Delta x}{2}\left(\cdots + u_{i-\frac{1}{2}} + u_{i,p} + u_{i+\frac{1}{2}} + u_{i+1,p} + \dots\right)$$

$$= \frac{\Delta x}{2}\left(\cdots + \left(\frac{1}{2}u_{i-\frac{1}{2}} + u_{i,p} + \frac{1}{2}u_{i+\frac{1}{2}}\right) + \left(\frac{1}{2}u_{i+\frac{1}{2}} + u_{i+1,p} + \frac{1}{2}u_{i+\frac{3}{2}}\right)\cdots\right).$$

Thus, the quadrature induced by the diagonal mass matrix M defined by (3.4) can be considered either as the chained trapezoidal rule on the complete computational domain or in each individual cell. In fact, transferred to the interface and midpoint nodes $u_i, u_{i,p}$ this quadrature rule directly corresponds to the diagonal mass matrix of the classical second-order SBP operator on equidistant nodes with grid spacing $\frac{\Delta x}{2}$. ◁

If we only focused on the central Active Flux method, we might stop here since diagonal norm/mass matrices offer the best structure for many types of equations, e.g., in the presence of variable coefficients or curved grids [59]. However, we are interested in the upwind version of the Active Flux method, as this version is more commonly used in practice. It will become clear in the following sections that we cannot use the diagonal mass matrix M (3.4) for the upwind case. Therefore, here, we continue to explore a more general class of mass matrices.

Among diagonal matrices, (3.4) is unique up to a scalar factor. Allowing for non-diagonal M, a mass matrix which induces the SBP property is not unique, as we can see in the following discussion. The additional parameters introduced here will be required for the upwind Active Flux method. Firstly, the following lemma shows the non-uniqueness of a symmetric mass matrix satisfying $MD = -D^T M$.

Lemma 3.3. *All the symmetric, pentadiagonal matrices (up to boundary terms) which ensure that the derivative operator D of the central semi-discrete Active Flux method* (3.3) *is skew-symmetric with respect to M, are of the form*

$$M = \Delta x \begin{pmatrix} & \ddots & & & & & \\ m_{vv} & \frac{m_v-3m_p}{2} & m_v & \frac{m_v-3m_p}{2} & m_{vv} & & \\ & \frac{3m_p-m_v+2m_{vv}}{6} & \frac{m_v-3m_p}{2} & m_p & \frac{m_v-3m_p}{2} & \frac{3m_p-m_v+2m_{vv}}{6} & \\ & & m_{vv} & \frac{m_v-3m_p}{2} & m_v & \frac{m_v-3m_p}{2} & m_{vv} \\ & & & & & \ddots & \end{pmatrix} \tag{3.6}$$

with $m_p, m_v, m_{vv} \in \mathbb{R}$.

Proof. Due to the alternate setting of point values and cell averages in the Active Flux method, we use the ansatz

$$M = \Delta x \begin{pmatrix} & \ddots & & & & \\ m_{vv} & m_{vp} & m_v & m'_{vp} & m_{vv} & \\ & m_{pp} & m'_{vp} & m_p & m_{vp} & m_{pp} \\ & & m_{vv} & m_{vp} & m_v & m'_{vp} & m_{vv} \\ & & & & & \ddots & \end{pmatrix}, \tag{3.7}$$

where m_v and m_p are on the diagonal of M corresponding to the cell average (volume) and the point values, respectively. The skew symmetry $MD + D^T M = 0$ requires

$$m'_{vp} - m_{vp} = 0, \tag{3.8}$$

$$3m_{pp} + m_{vp} - m_{vv} = 0, \tag{3.9}$$

$$3m_p - 3m_{pp} + m'_{vp} - m_v + m_{vv} = 0, \tag{3.10}$$

from which we directly obtain $m'_{vp} = m_{vp}$. Using this and adding the last two equations (3.9), (3.10) we can solve for m_{vp} and then for m_{pp}. Thus, we obtain

$$m_{pp} = \frac{3m_p - m_v + 2m_{vv}}{6}, \quad m_{vp} = \frac{m_v - 3m_p}{2}, \tag{3.11}$$

which leaves us with the structure of M as presented in (3.6). □

Remark 3.4. The banded mass matrix (3.6) reduces to the diagonal mass matrix in (3.4) for $m_{vv} = 0$, $m_p = m_v/3$, and $m_v = \frac{3}{4}$. ◁

Secondly, for the matrix M in (3.6) to qualify as a mass matrix of an SBP operator, we require M to be positive definite. In the following, we restrict the investigation to $m_{vv} = 0$, since this will be required later for the upwind version of Active Flux method. Moreover, setting $m_{vv} \neq 0$ would result in a bigger stencil of M in comparison to the stencil of the derivative operators. The following lemma determines a range of parameters for which M is positive definite and gives one case of a positive semidefinite M with multiplicity one of the corresponding zero eigenvalue.

Lemma 3.5. *For $m_{vv} = 0$, the matrix M in* (3.6) *has the following properties.*

1. *If $2m_v/9 < m_p < 2m_v/3$ and $m_v > 0$, then M is positive definite.*
2. *If $m_p = 2m_v/9$ and $m_v > 0$ then M is positive semidefinite with an eigenvalue 0 of multiplicity 1.*

The technical proof of Lemma 3.5 involving properties of circulant matrices can be found in Appendix A.

For $m_{vv} = 0$ and $m_p \neq 2m_v/3$, it is possible to rescale the matrix M in (3.6) to satisfy the classical constraint $\mathbf{1}^T M \mathbf{1} = x_{\max} - x_{\min}$. Thus, we obtain

Theorem 3.6. *The central version* (2.10) *of the semi-discrete Active Flux method can be formulated using SBP operators with derivative matrix*

$$D = \frac{1}{\Delta x}\begin{pmatrix} \ddots & & & & & & \\ -1 & 0 & 1 & & & & \\ 1 & -3 & 0 & 3 & -1 & & \\ & & -1 & 0 & 1 & & \\ & & 1 & -3 & 0 & 3 & -1 \\ & & & & -1 & 0 & 1 \\ & & & & & & \ddots \end{pmatrix}, \tag{3.12}$$

and positive definite mass matrix

$$M = \frac{3\Delta x}{8m_v - 12m_p}\begin{pmatrix} \ddots & & & & & \\ \frac{m_v-3m_p}{2} & m_v & \frac{m_v-3m_p}{2} & & & \\ \frac{3m_p-m_v}{6} & \frac{m_v-3m_p}{2} & m_p & \frac{m_v-3m_p}{2} & \frac{3m_p-m_v}{6} & \\ & & \frac{m_v-3m_p}{2} & m_v & \frac{m_v-3m_p}{2} & \\ & & & & \ddots & \end{pmatrix}, \tag{3.13}$$

for $m_v > 0$ and $2m_v/9 < m_p < 2m_v/3$, satisfying $\mathbf{1}^T M \mathbf{1} = x_{\max} - x_{\min}$.

Next, we will use the additional degrees of freedom introduced by the banded structure of the mass matrix M in Theorem 3.6 to generalize the results to the upwind version of the Active Flux method.

3.2. Upwind version of the Active Flux method

We first collect the formulas for the upwind semi-discrete Active Flux method. The cell average update is

$$\frac{\mathrm{d}}{\mathrm{d}t}u_i + \frac{u_{i+1/2} - u_{i-1/2}}{\Delta x} = 0, \tag{3.14}$$

the upwind point value update for positive advection velocity (see (2.8)) is

$$\frac{\mathrm{d}}{\mathrm{d}t}u_{i+1/2} + \frac{2u_{i-1/2} - 6u_i + 4u_{i+1/2}}{\Delta x} = 0, \tag{3.15}$$

and for negative advection velocity (see (2.9)), we have

$$\frac{\mathrm{d}}{\mathrm{d}t}u_{i+1/2} - \frac{-4u_{i+1/2} + 6u_{i+1} - 2u_{i+3/2}}{\Delta x} = 0. \tag{3.16}$$

The upwind versions of the Active Flux method correspond to the derivative operators

$$D_+ = \frac{1}{\Delta x}\begin{pmatrix} \ddots & & & & & \\ -1 & 0 & 1 & & & \\ & & -4 & 6 & -2 & \\ & & -1 & 0 & 1 & \\ & & & & -4 & 6 & -2 \\ & & & & -1 & 0 & 1 \\ & & & & & & \ddots \end{pmatrix}, \quad D_- = \frac{1}{\Delta x}\begin{pmatrix} \ddots & & & & & \\ -1 & 0 & 1 & & & \\ 2 & -6 & 4 & & & \\ & & -1 & 0 & 1 & \\ & & 2 & -6 & 4 & \\ & & & & -1 & 0 & 1 \\ & & & & & & \ddots \end{pmatrix}. \tag{3.17}$$

Unfortunately, these operators are not SBP operators with the diagonal mass matrix (3.4). However we can still achieve this property using a banded mass matrix as for the central approximation above. In addition, restricting the band width of the mass matrix to the band width of the derivative operators results in uniqueness of the admissible mass matrix M up to a scalar factor.

Lemma 3.7. *The symmetric matrix*

$$M = \Delta x\begin{pmatrix} \ddots & & & & & \\ 0 & -m_v/2 & m_v & -m_v/2 & 0 & \\ & m_v/6 & -m_v/2 & 2m_v/3 & -m_v/2 & m_v/6 \\ & & 0 & -m_v/2 & m_v & -m_v/2 & 0 \\ & & & & & \ddots \end{pmatrix} \tag{3.18}$$

is — up to a scalar factor $m_v \in \mathbb{R}$ — the only symmetric matrix which is pentadiagonal (up to boundary terms) and ensures that the derivative operators $D_\pm$ of the upwind semi-discrete Active Flux method (3.17) *are adjoint to each other with respect to M.*

Proof. We use the same ansatz as for the proof of Lemma 3.3. Then, the mutual adjointness $MD_+ + D_-^T M = 0$ requires $m_{vv} = 0$ and

$$m_{vp} - m'_{vp} = 0 \qquad 6m_{pp} + 4m'_{vp} + m_v = 0 \tag{3.19}$$

$$6m_p + 4m_{vp} - m_v + 2m'_{vp} = 0 \qquad 6m_{pp} + 2m_{vp} = 0 \tag{3.20}$$

This yields $m_{vp} = m'_{vp} = -m_v/2,\ m_p = 2m_v/3,\ m_{pp} = m_v/6$ and hence (3.18). □

Remark 3.8. Note that the matrix M in (3.18) is a special case of the matrix in (3.6) with $m_p = 2m_v/3$. In this case, M is positive semidefinite as shown in the following lemma. ◁

Lemma 3.9. *The matrix M in* (3.18) *is positive semidefinite for $m_v > 0$ with an eigenvalue 0 of multiplicity 1 and eigenvector* $\mathbf{1}$.

Proof. A simple calculation shows that the rows of M sum up to zero. Thus, $\mathbf{1}$ is an eigenvector of M with eigenvalue 0. It is sufficient to consider the case $m_v = 1$ to study its multiplicity and to

determine the sign of the other eigenvalues. Using Lemma A.1, the matrix B_k associated with M for $m_v = 1$ is given by (with $\theta = \frac{2\pi k}{n}$, $k = 0, \dots, n-1$)

$$B_k = \begin{pmatrix} 1 & -(1+e^{-i\theta})/2 \\ -(1+e^{i\theta})/2 & (2+\cos\theta)/3 \end{pmatrix} \tag{3.21}$$

and its characteristic polynomial is

$$z^2 - \frac{z}{3}(5+\cos\theta) + \frac{1}{6}(1-\cos\theta). \tag{3.22}$$

Its value at $z = 0$ can only vanish if $\theta = 0$. Thus, this eigenvalue only appears once. Furthermore, for $\theta \in (0, 2\pi)$, the eigenvalues are positive since the roots of the characteristic polynomial are given by $z_{1,2} = \frac{1}{6}\left(\cos\theta + 5 \pm \sqrt{(\cos\theta+5)^2 - 6(1-\cos\theta)}\right) > 0$. □

Remark 3.10. Classical finite difference SBP operators have the scaling $D \propto \Delta x^{-1}$ and $M \propto \Delta x$. Remark 3.2 demonstrates that this expected scaling of the mass matrix M also holds for the central Active Flux method. However, we cannot obtain the scaling $M \propto \Delta x$ by imposing $\mathbf{1}^T M \mathbf{1} = x_{\max} - x_{\min}$ since $M\mathbf{1} = \mathbf{0}$ for the upwind Active Flux method. Thus, we need to consider another way to fix the free parameter m_v in (3.18). To do so, we introduce the vector $\mathbf{1}_{\text{avg}} = (\dots, 0, 1, 0, 1, \dots)^T$ which has a value unity for all averages and zero for all point values. Then, we compute

$$\frac{\mathbf{1}_{\text{avg}}^T M \boldsymbol{u}}{\Delta x\, m_v} = \cdots + u_{i-2} - u_{i-\frac{3}{2}} + u_{i-1} - u_{i-\frac{1}{2}} + u_i - u_{i+\frac{1}{2}} + u_{i+1} - \dots$$

In particular, we can choose $\boldsymbol{u} = \mathbf{1}_{\text{avg}}$, resulting in

$$\frac{\mathbf{1}_{\text{avg}}^T M \mathbf{1}_{\text{avg}}}{\Delta x\, m_v} = \cdots + u_{i-2} + u_{i-1} + u_i + u_{i+1} + \cdots = \frac{x_{\max} - x_{\min}}{\Delta x}.$$

This shows that choosing $m_v = 1$ yields $\mathbf{1}_{\text{avg}}^T M \mathbf{1}_{\text{avg}} = x_{\max} - x_{\min}$, i.e., the expected scaling of the mass matrix $M \propto \Delta x$ (when focusing only on the volume contributions). ◁

Relaxing the definiteness condition to allow for a positive semidefinite mass matrix M still enables a stability proof for the Active Flux method via SBP properties as we will show in section 4. At this point however, we still need to prove the upwind SBP property requiring that $M(D_+ - D_-)$ is negative semidefinite. This is the subject of the following lemma.

Lemma 3.11. *For M in* (3.18) *and the upwind operators $D_\pm$ in* (3.17)*, the matrix $M(D_+ - D_-)$ is symmetric and negative semidefinite for $m_v > 0$.*

Proof. Concerning the symmetry, we have

$$\frac{M(D_+ - D_-)}{m_v} = \begin{pmatrix} & & \ddots & & & & & & & & & \\ \hline \dots & -8/3 & 5 & -6 & 5 & -8/3 & 1 & -1/3 & & & & \\ \dots & 1 & -3 & 5 & -6 & 5 & -3 & 1 & 0 & & & \\ \hline & -1/3 & 1 & -8/3 & 5 & -6 & 5 & -8/3 & 1 & -1/3 & & \\ & & 0 & 1 & -3 & 5 & -6 & 5 & -3 & 1 & 0 & \\ \hline & & & -1/3 & 1 & -8/3 & 5 & -6 & 5 & -8/3 & 1 & -1/3 & \\ & & & & 0 & 1 & -3 & 5 & -6 & 5 & -3 & 1 & 0 \\ \hline & & & & & & & & & \ddots & & & \end{pmatrix}. \tag{3.23}$$

Finally, using Lemma A.1, one finds, calling $\theta := \frac{2\pi k}{n}$, $k = 0, \dots, n-1$, the eigenvalues $\lambda(\theta)$ to be 0 (n times) and

$$\lambda(\theta) = -\frac{2}{3}\left(18 + 17\cos\theta + \cos(2\theta)\right) < 0, \qquad \forall\theta. \tag{3.24}$$

□

Remark 3.12. Following the nomenclature introduced in [28] for central SBP operators, we combine the previous results (Lemma 3.7, Lemma 3.9, and Lemma 3.11) and say that the semi-discrete Active Flux upwind operators $D_\pm$ are *degenerate* upwind SBP operators when combined with the semidefinite mass matrix M (3.18). ◁

4. Stability of the Active Flux method via SBP properties

Since the central version of the Active Flux method can be formulated using SBP operators, we directly obtain stability.

Corollary 4.1. *The central version* (2.10) *of the semi-discrete Active Flux method is stable for the linear advection* (2.2) *with periodic boundary conditions.*

Proof. This follows immediately from Theorem 3.6 and classical stability properties of SBP operators. □

Unfortunately, the matrix M for which the upwind Active Flux operators $D_\pm$ are mutually adjoint is only positive semidefinite. Thus, the classical energy stability proof does not guarantee stability immediately. However, based on Lemma 3.9, we can still obtain a stability result for the Active Flux method using the framework of SBP operators.

The idea is as follows. We show below that the states associated to zero energy are uniform (in space) constants. Thus, if the energy is decaying, it is, generally speaking, possible that a uniform constant could grow: our mass matrix has constants in its kernel and its energy is zero. However, the time evolution of uniform constants is easy to check separately, and we find that uniform constants do not grow in time.

Theorem 4.2. *The upwind Active Flux semi-discretization*

$$\frac{\mathrm{d}}{\mathrm{d}t}\boldsymbol{u} + D_-\boldsymbol{u} = \mathbf{0} \tag{4.1}$$

using (3.14) *and* (2.8) *of the linear advection equation* (2.2) *with* $a = 1$ *with periodic boundary conditions is stable.*

Proof. Using Lemma 3.9, we decompose the vector $\boldsymbol{u} = \boldsymbol{u}_0 + \boldsymbol{u}_\perp$ into the components $\boldsymbol{u}_0 \propto \mathbf{1}$ in the kernel of M and $\boldsymbol{u}_\perp \perp \mathbf{1}$ in its orthogonal complement. Following the usual upwind SBP argumentation (2.20), we obtain

$$\frac{\mathrm{d}}{\mathrm{d}t}\|\boldsymbol{u}\|_M^2 = 2\boldsymbol{u}^T M\frac{\mathrm{d}}{\mathrm{d}t}\boldsymbol{u} = -2\boldsymbol{u}^T M D_-\boldsymbol{u} = -\boldsymbol{u}^T M D_-\boldsymbol{u} + \boldsymbol{u}^T D_+^T M\boldsymbol{u} \le 0, \tag{4.2}$$

where we have used Lemma 3.11. Since $M\mathbf{1} = \mathbf{0}$, $\|\boldsymbol{u}\|_M = \|\boldsymbol{u}_\perp\|_M$ and the component in the orthogonal complement is stable. The component in the kernel of M is constant in time and thus also stable, since

$$\frac{\mathrm{d}}{\mathrm{d}t}\boldsymbol{u}_0 = -D_-\boldsymbol{u}_0 = \mathbf{0}. \tag{4.3}$$

Thus, the method is stable. □

The Theorem and Proof above hold analogously for the linear advection equation (2.9) with the opposite speed when using D_+.

5. Numerical experiment

To exemplify the theoretical stability results, we perform a numerical experiment based on the linear advection equation $\partial_t u + \partial_x u = 0$ with periodic boundary conditions in the interval $[0, 2\pi]$ and the initial condition $u(0, x) = \exp(\sin(x))$. We use the central and upwind semi-discrete Active Flux methods with 10 and 50 volumes, respectively, and integrate the resulting ODE system in time using the five-stage, third-order explicit Runge-Kutta method RK3(2)5$_F$[3S$^*_+$] of [46] with time step size $\Delta t = \Delta x/2$. We chose this method since it has been optimized for hyperbolic problems and includes an interval on the imaginary axis in its stability interval as required for stability of central operators.

The energy analysis presented in the previous sections concentrates on the effect of the spatial semi-discretization. When integrating the resulting ODE in time, the energy behavior also depends on the time integration scheme. While many explicit Runge-Kutta methods can be shown to add additional dissipation for linear problems [50, 57, 58, 63]. As a remark, we mention here that the analysis of nonlinear problems is more complex [35, 45, 47]. Since we are interested in a quadratic energy, we could use a symplectic Runge-Kutta method such as the implicit midpoint rule to preserve the energy evolution caused by the semi-discretization in space, cf. sections IV.2.1 and IV.4.1 of [27]. However, we would like to avoid introducing fully implicit methods for hyperbolic problems. Thus, we apply the relaxation approach discussed and analyzed in [32, 48, 52] to modify an explicit Runge-Kutta method slightly so that the fully discrete energy evolution is purely caused by the spatial semi-discretization without additional influence of the time integration method. To demonstrate the dissipative effect of the time integration method, we also show results without relaxation in time.

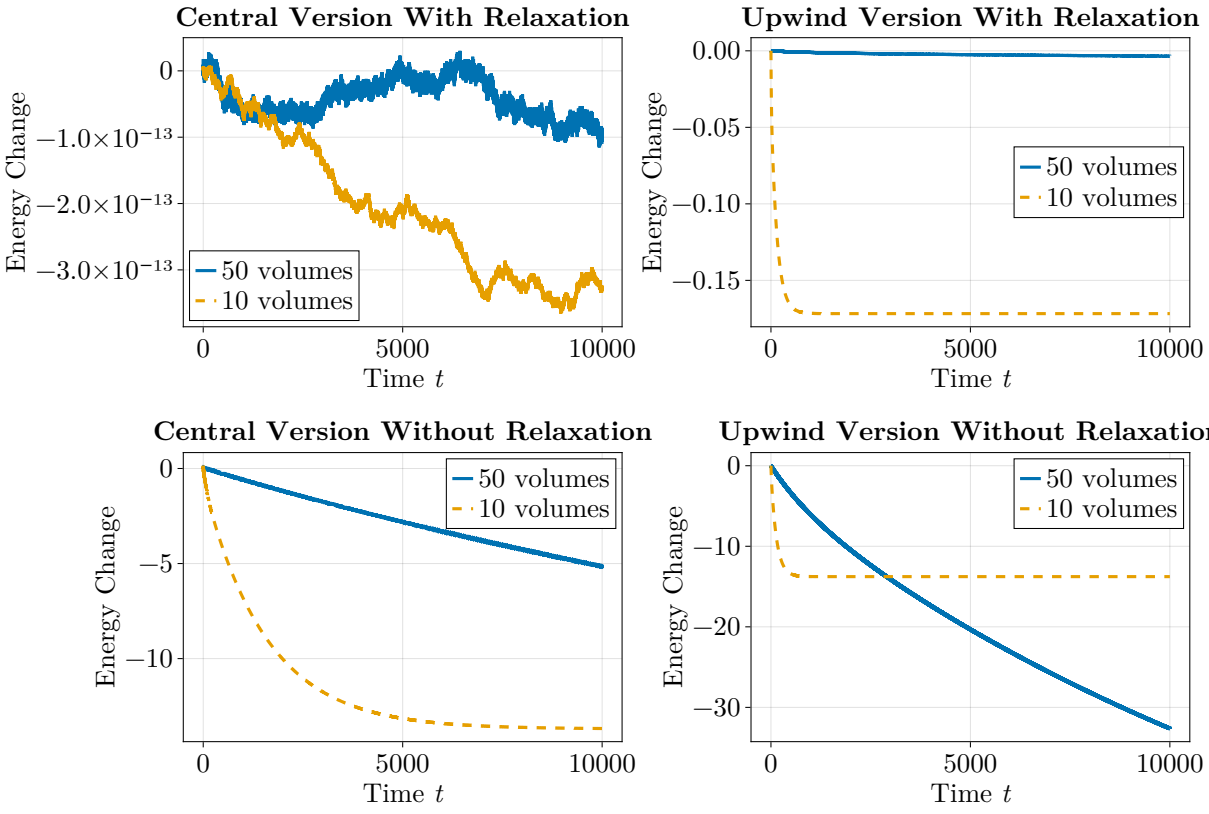

Figure 2: Change of the discrete energy $\|\boldsymbol{u}\|_M^2 = \boldsymbol{u}^T M \boldsymbol{u}$ compared to the initial energy. For the central version, we use the diagonal mass matrix (3.4); for the upwind version, we use the pentadiagonal (up to boundary terms) mass matrix (3.18) with $m_v = 1$.

The results are shown in Figure 2. In accordance with the theory, the energy is conserved up

to roundoff errors for the central version while the upwind version results in energy dissipation if relaxation in time is used. Without relaxation, the explicit time integration method introduces additional dissipation. All Julia [11] code and instructions required to reproduce these numerical experiments are available in our reproducibility repository [10]. We used CairoMakie.jl [15] to create the figures.

6. Nullspace consistency of the Active Flux upwind SBP operator

An additional property of the Active Flux difference operators which is not directly related to their upwind SBP property is nullspace consistency. This property is interesting on its own merit since it transfers an additional algebraic property from the continuous to the discrete setting. Nullspace consistency is a rather recently studied mimetic property in the context of derivative operators and numerical methods for PDEs. It signifies that the nullspace of the continuous operator is correctly transferred to its discrete counterpart. In the context of SBP schemes, this concept was first introduced in [61], connected to the investigation of convergence rates of FD schemes. According to the definition of nullspace consistency, for a nullspace consistent finite difference operator D_k approximating the continuous operator ∂_x^k, the kernel of D_k can be mapped one-to-one to the kernel of ∂_x^k.

In the context of periodic problems such as those studied in this work, nullspace consistency prevents spurious modes, that are contained in the discrete kernel of D_k but not in its continuous counterpart, from persisting in the numerical solution for all times. In the absence of round-off and cancellation errors, such spurious modes are unaffected by the numerical scheme and remain constant in time, since the discrete derivative operator maps them to zero. A spurious mode may hence exist in the initial data, e.g. in an underresolved simulation, or be created due to round-off errors. The continuous linear advection equation transports this mode at the speed determined by the advection coefficient, while the semi-discrete scheme leaves it unchanged in time. Since we have a linear problem, due to energy stability, such modes will not get amplified since their energy cannot grow. However, if the scheme is not nullspace consistent, there is also no dissipation mechanism which can damp out this spurious high-frequency mode in the periodic setting. In contrast, nullspace consistency allows for such a damping mechanism. The following lemma shows that upwind Active Flux difference operators are nullspace consistent.

Lemma 6.1. *The Active Flux difference operators D_- and D_+ are nullspace consistent, i.e., $D_\pm \boldsymbol{u} = \mathbf{0} \iff \boldsymbol{u} \propto \mathbf{1}$.*

Proof. Due to symmetry, it is sufficient to consider D_- as the proof for D_+ follows analogously. The nullspace of the linear continuous operator ∂_x consists of the functions constant in x. Thus, we require that the only vectors $\boldsymbol{u}$ satisfying $D_-\boldsymbol{u} = \mathbf{0}$ are the constants $\boldsymbol{u} = c\mathbf{1}$.

Obviously, all vectors of the form $\boldsymbol{u} = c\mathbf{1}$ satisfy $D_-\boldsymbol{u} = \mathbf{0}$. It remains to show that all the vectors $\boldsymbol{u}$ with $D_-\boldsymbol{u} = \mathbf{0}$ are of the form $\boldsymbol{u} = c\mathbf{1}$. Then, all vectors in the nullspace of D_- have a counterpart in the nullspace of ∂_x. The linear difference scheme resulting from the condition $D_-\boldsymbol{u} = \mathbf{0}$ is

$$\begin{aligned} \forall i: \quad & -u_{i-\frac{1}{2}} + u_{i+\frac{1}{2}} = 0, \\ \forall i: \quad & 2u_{i-\frac{1}{2}} - 6u_i + 4u_{i+\frac{1}{2}} = 0. \end{aligned}$$

From the first equation, we obtain the existence of a constant $c \in \mathbb{R}$ such that $u_{i+\frac{1}{2}} = c$ is constant for all i. Inserting this into the second equation then yields $u_i = c$ for all i, i.e., $\boldsymbol{u} = c\mathbf{1}$. □

The central version of the Active Flux method is not nullspace consistent. This is in line with the lack of nullspace consistency for periodic problems of the classical central second-order finite difference operator approximating the first derivative based on the approximation $\partial_x u(x_i) \approx \frac{u_{i+1} - u_{i-1}}{2\Delta x}$.

Lemma 6.2. *The central Active Flux difference operator D in* (3.3) *has a two-dimensional nullspace spanned by the vectors* $\mathbf{1}$ *and* $(1,-1,1,-1,\dots,1,-1)^T$*. Therefore, the central version* (2.10) *of the Active Flux method is not nullspace consistent.*

Proof. As before, all vectors of the form $\boldsymbol{u} = c\mathbf{1}$ obviously satisfy $D\boldsymbol{u} = \mathbf{0}$. Furthermore, the linear difference scheme resulting from the condition $D\boldsymbol{u} = \mathbf{0}$ is given by

$$\begin{aligned} \forall i: \qquad & -u_{i-\frac{1}{2}} + u_{i+\frac{1}{2}} = 0, \\ \forall i: \qquad & u_{i-\frac{1}{2}} - 3u_i + 3u_{i+1} - u_{i+\frac{3}{2}} = 0. \end{aligned}$$

From the first equation, we again obtain that $u_{i+\frac{1}{2}} = c$ is constant for all i. Inserting this into the second equation now yields $u_{i+1} = u_i = d$ for all i, for a potentially different constant d. Setting $c = 1$ and $d = \pm 1$ we obtain the two linearly independent vectors $\mathbf{1}$ and $(1,-1,1,-1,\dots,1,-1)^T$ which span the nullspace of D. □

Remark 6.3. On finite non-periodic domains, nullspace consistency for central difference approximations can be restored by suitable boundary closures [61]. ◁

Remark 6.4. The lack of nullspace consistency is not specific to the central Active Flux method, but just a consequence of its central character. Indeed, it is well-known that any periodic SBP operator with an even number of degrees of freedom is not nullspace consistent: A periodic SBP operator is skew symmetric (with respect to the inner product induced by the mass matrix). Thus, it is unitarily diagonalizable, all eigenvalues are on the imaginary axis, and eigenvalues are either real or come in complex conjugate pairs. Zero is an eigenvalue because of consistency of the SBP operator (mapping constants to zero). Thus, if a periodic SBP operator has an even number of degrees of freedom, it needs to have an eigenspace associated to the eigenvalue zero of dimension at least two. For example, all central finite difference operators with an even number of nodes have grid oscillations $(1,-1,1,-1,\dots,1,-1)^T$ in their nullspace. Fourier collocation methods map such grid oscillations (the Nyquist frequency) to zero as well. ◁

7. Summary

To the best of our knowledge, we have proven stability using the summation-by-parts technique for an Active Flux method for the first time. To this end, we considered the linear advection equation on an interval with periodic boundary conditions. The Active Flux method, a finite volume method based on a globally continuous approach, combines cell average updates with point updates at the cell edges. We have studied two ways of updating the point values. First the point value updates using a *central discretization* (2.11) are chosen for purposes of theoretical analysis in section 3.1. In section 3.2 the commonly used *upwind* (see (2.8) and (2.9)) version of the point value update is considered. Stability is shown for both cases in section 4. In Section 5, we provide numerical examples illustrating stability, consistent with the theoretical results in this paper. In Section 6, we showed that the upwind Active Flux method is nullspace consistent while the central one is not. As an additional bonus, the relation between energy stability via summation by parts and von Neumann stabiliy is shown in section B for our PDE at hand.

Acknowledgments

The authors acknowledge funding by the Deutsche Forschungsgemeinschaft (DFG, German Research Foundation) within *SPP 2410 Hyperbolic Balance Laws in Fluid Mechanics: Complexity, Scales, Randomness (CoScaRa)*, project numbers 525941602 (W.B., C.K., L.L.), 526073189 (S.O.) and 526031774 (H.R.). H.R. additionally acknowledges the DFG individual research grant 513301895. J.N. was supported by Vetenskapsrådet, Sweden [no. 2021-05484 VR] and University of Johannesburg Global Excellence and Stature Initiative Funding.

A. Properties of block circulant matrices and Proof of Lemma 3.5

Block circulant matrices [16, 64] are an extension of circulant matrices and possess the general form

$$A = \begin{pmatrix} A_0 & A_1 & & & A_{n-1} \\ A_{n-1} & A_0 & A_1 & & \\ & A_{n-1} & A_0 & A_1 & \\ & & & \ddots & \\ A_1 & & & A_{n-1} & A_0 \end{pmatrix} \in \mathbb{R}^{nm \times nm}, \tag{A.1}$$

with $A_k \in \mathbb{R}^{m \times m}$ for $k = 0, \ldots, n-1$.

The semi-discrete Active Flux method in one space dimension on a periodic domain yields block circulant matrices D_+, D_- and M and consequently also $M(D_+ - D_-)$ has a block circulant structure. Due to the alternating difference formulas for point values and for cell averages, the involved matrices hereby possess a specific structure of 2×2 subblocks

$$A_k = \begin{pmatrix} a_k & a_{k+1} \\ b_k & b_{k+1} \end{pmatrix}, \quad k = 0, \ldots, n-1.$$

We may thus exploit the theory of block circulant matrices to obtain eigenvalues and eigenvectors of the given matrices.

Lemma A.1 (Eigenvalues of block circulant matrices). *The eigenvalues of the $nm \times nm$ matrix* (A.1) *are the eigenvalues of all matrices*

$$B_k = A_0 + r^k A_1 + \ldots r^{k(n-1)} A_{n-1}, \qquad k = 0, 1, \ldots, n-1, \tag{A.2}$$

with $r = \mathrm{e}^{2\pi \mathrm{i}/n}$ the roots of unity. If λ is an eigenvalue of B_k with corresponding eigenvector v, then λ is also an eigenvalue of A with eigenvector $(v^{\mathrm{T}}, r^k v^{\mathrm{T}}, r^{2k} v^{\mathrm{T}}, \ldots, r^{(n-1)j} v^{\mathrm{T}})^{\mathrm{T}}$.

Proof. Consider the following ansatz for an eigenvector of A

$$e_k = (v^{\mathrm{T}}, r^k v^{\mathrm{T}}, r^{2k} v^{\mathrm{T}}, \ldots, r^{(n-1)j} v^{\mathrm{T}})^{\mathrm{T}}, \qquad k = 0, 1, \ldots, n-1, \tag{A.3}$$

for some yet to be determined $v \in \mathbb{C}^m$. Then, $Ae_k = \lambda_k e_k$ if

$$Ae_k = \begin{pmatrix} A_0 v + r^k A_1 v + \ldots + r^{(n-2)k} A_{n-2} v + r^{(n-1)k} A_{n-1} v \\ A_{n-1} v + r^k A_0 v + r^{2k} A_1 v + \ldots + r^{(n-1)k} A_{n-2} v \\ \vdots \\ A_1 v + \ldots + r^{(n-3)k} A_{n-2} v + r^{(n-2)k} A_{n-1} v + r^{(n-1)k} A_0 v \end{pmatrix} = \lambda_k \begin{pmatrix} v \\ r^k v \\ \vdots \\ r^{(n-1)k} v \end{pmatrix}. \tag{A.4}$$

The i-th component of this equation is ($i = 0, \ldots, n-1$)

$$\sum_{j=n-i}^{n-1} r^{(j-n+i)k} A_j v + r^{ik} \sum_{j=0}^{n-1-i} r^{jk} A_j v = \lambda_k r^{ik} v, \tag{A.5}$$

which reduces to just one equation for all i upon the choice $r = \exp\left(\frac{2\pi \mathrm{i}}{n}\right)$. Then, the eigenvalue problem reduces to

$$\sum_{j=0}^{n-1} r^{jk} A_j v = B_k v = \lambda_k v. \tag{A.6}$$

□

As shown in [64], all eigenvalues and eigenvectors of A can be obtained in this manner. In addition, while all circulant matrices can be diagonalized, block circulant matrices allow for block diagonalization. A block circulant matrix does not necessarily possess a complete set of linearly independent eigenvectors; however, it does so if the matrices B_k can all be diagonalized. In this case, the block circulant matrix can be diagonalized as well.

Lemma A.2. *Let $F \in \mathbb{C}^{n\times n}$ be the unitary matrix with entries $F_{jk} = \frac{1}{\sqrt{n}} r^{(j-1)(k-1)}$, $r = e^{2\pi \mathrm{i}/n}$, and $I_m = \mathrm{diag}(1,\dots,1) \in \mathbb{R}^{m\times m}$. For a block circulant matrix $A \in \mathbb{R}^{mn\times mn}$ as in* (A.1)*, we have*

$$(F^* \otimes I_m) A (F \otimes I_m) = \mathrm{diag}(B_0, \dots, B_{n-1}), \tag{A.7}$$

with B_k, $k = 0,\dots,n-1$ given in (A.2)*.*

Proof. Using

$$F \otimes I_m = \frac{1}{\sqrt{n}} \begin{pmatrix} I_m & I_m & I_m & \cdots & I_m \\ I_m & rI_m & r^2 I_m & \cdots & r^{n-1} I_m \\ I_m & r^2 I_m & r^4 I_m & \cdots & r^{2(n-1)} I_m \\ \vdots & & \vdots & & \\ I_m & r^{n-1} I_m & r^{2(n-1)} I_m & \cdots & r^{(n-1)^2} I_m \end{pmatrix}$$

and $r^n = 1$, we first obtain

$$A(F \otimes I_m) = \frac{1}{\sqrt{n}} \begin{pmatrix} B_0 & B_1 & B_2 & \cdots & B_{n-1} \\ B_0 & B_1 r & B_2 r^2 & \cdots & B_{n-1} r^{n-1} \\ \vdots & & & & \vdots \\ B_0 & B_1 r^{n-1} & B_2 r^{2(n-1)} & \dots & B_{n-1} r^{(n-1)^2} \end{pmatrix}$$

with B_k given in (A.2). Using $F^*_{jk} = \frac{1}{\sqrt{n}} \bar{r}^{(j-1)(k-1)}$ with $\bar{r} = e^{-2\pi \mathrm{i}/n}$, i.e.,

$$F^* \otimes I_m = \frac{1}{\sqrt{n}} \begin{pmatrix} I_m & I_m & I_m & \cdots & I_m \\ I_m & \bar{r} I_m & \bar{r}^2 I_m & \cdots & \bar{r}^{n-1} I_m \\ I_m & \bar{r}^2 I_m & \bar{r}^4 I_m & \cdots & \bar{r}^{2(n-1)} I_m \\ \vdots & & \vdots & & \\ I_m & \bar{r}^{n-1} I_m & \bar{r}^{2(n-1)} I_m & \cdots & \bar{r}^{(n-1)^2} I_m \end{pmatrix},$$

we have

$$(F^* \otimes I_m) A (F \otimes I_m) = \frac{1}{n} \begin{pmatrix} nB_0 & p(r)B_1 & p(r^2)B_2 & \cdots & p(r^{n-1})B_{n-1} \\ p(r^{n-1})B_0 & nB_1 & p(r)B_2 & \cdots & p(r^{n-2})B_{n-1} \\ \vdots & & & \dots & \vdots \\ p(r)B_0 & p(r^2)B_1 & p(r^3)B_2 & \cdots & nB_{n-1} \end{pmatrix},$$

with $p(z) = 1 + z + z^2 + \ldots + z^{n-1}$, where we exploit $\bar{r}^k = r^{n-k}$. Finally, for $z = r^k$ with $k \neq 0$ we have $p(z) = 0$, since the values r^k, $k = 1,\dots,n-1$ are the roots of $z^n = 1$ which differ from $z = 1$ and we may factorize $z^n - 1 = (z-1)(1 + z + z^2 + \ldots + z^{n-1})$. Thus, the block-diagonal form (A.7) is proven. □

Proof of Lemma 3.5. We use Lemma A.1 and the notation described there. The eigenvalues of M can then be determined by the eigenvalues of the matrices B_k which in this case are given by

$$B_k = \begin{pmatrix} m_p + 2m_{pp}\cos\theta & m_{vp}\left(1 + e^{-\mathrm{i}\theta}\right) \\ m_{vp}\left(1 + e^{\mathrm{i}\theta}\right) & m_v \end{pmatrix}, \quad \theta := \frac{2\pi k}{n}, \tag{A.8}$$

with m_{pp} and m_{vp} determined by (3.11). The characteristic polynomial p of B_k is given by

$$p(z) = z^2 - tz + d \tag{A.9}$$

with t and d the trace and determinant of B_k, respectively,

$$t = \operatorname{trace}(B_k) = \frac{1}{3}\left(3(m_p + m_v) + (3m_p - m_v)\cos\theta\right), \tag{A.10}$$

$$d = \det B_k = \frac{1}{6}\left(-3(9m_p^2 - 8m_p m_v + m_v^2) - (9m_p - 5m_v)(3m_p - m_v)\cos\theta\right). \tag{A.11}$$

We are now interested in a range of parameters m_v, m_p for which B_k has only positive eigenvalues for any value of θ. From the solution formula of quadratic equations it is clear that for positive solutions one requires $t > 0$ and $d > 0$ which yields the following inequalities regarding the coefficients of the characteristic polynomial:

$$3(m_p + m_v) + (3m_p - m_v)\cos\theta > 0, \tag{A.12}$$

$$-3(9m_p^2 - 8m_p m_v + m_v^2) - (9m_p - 5m_v)(3m_p - m_v)\cos\theta > 0. \tag{A.13}$$

The latter inequality can be rewritten as

$$m_v^2 - (9m_p - 2m_v)(3m_p - 2m_v) - \left((9m_p - 2m_v)(3m_p - 2m_v) + m_v^2\right)\cos\theta > 0 \tag{A.14}$$

i.e.

$$m_v^2 - s - \left(s + m_v^2\right)\cos\theta > 0 \tag{A.15}$$

with $s := (9m_p - 2m_v)(3m_p - 2m_v)$. For $m_v > 0$, we obtain $s < 0$ precisely for $2m_v/9 < m_p < 2m_v/3$. In that case, by the strict triangle inequality, we have

$$|s + m_v^2| < |s| + m_v^2 = m_v^2 - s. \tag{A.16}$$

Since the condition $a + b\cos\theta > 0$ for all θ is equivalent to $|b| < a$, one thus has proven (A.13) for the range of parameters considered in the first statement of the Lemma. Furthermore, simply with $m_p, m_v > 0$ one obtains

$$|3m_p - m_v| \leq 3|m_p| + |m_v| < 3(m_p + m_v) \tag{A.17}$$

and thus (A.12) by the same argument. Thereby, we have proven the assertion that M possesses only positive eigenvalues if $m_v > 0$ and $2m_v/9 < m_p < 2m_v/3$.

Finally considering the case of positive semidefinite matrices M, we note that the characteristic polynomial p may have a zero eigenvalue, which is the case if and only if $d = \det B_k = 0$. For instance, this happens if

- $\theta = 0$ and either $m_p = \frac{2m_v}{9}$ or $m_p = \frac{2m_v}{3}$,
- $\theta = \pm\frac{\pi}{2}$ and $m_p = \frac{4\pm\sqrt{7}}{9}m_v = \begin{cases} 0.738...m_v > \frac{2}{3}m_v\,, \\ 0.150...m_v < \frac{2}{9}m_v\,. \end{cases}$

Analogously, other values of θ will likewise yield parameter values with B_k possessing a zero eigenvalue but will not be further studied here.

Considering the case $m_p = \frac{2m_v}{9}$, we have $\det B_k = \frac{1}{6}m_v^2(1 - \cos\theta)$, which only vanishes for $\theta = 0$, and since we have $\operatorname{trace}(B_k) \neq 0$ for $\theta = 0$, $m_p = \frac{2m_v}{9}$, the eigenvalue 0 has multiplicity 1. This proves the second statement of this lemma. The case $m_p = \frac{2m_v}{3}$ is treated in Lemma 3.7. □

B. Relation to von Neumann stability

Von Neumann stability uses the Fourier transform to make statements about the behavior in time of the L^2 norm of the solution. In its restricted setting of linear problems on periodic domains it can also be used to derive a mass matrix that satisfies the periodic SBP property, as will be shown now.

B.1. General theory

Since in the setting of the Active Flux method, cell averages and point values are independent degrees of freedom, and since their nature and their update equations differ, when performing von Neumann stability analysis they need to be associated to independent Fourier modes. We thus write

$$u_j = \sum_\omega \hat{u}^{\text{avg}}(\omega) \exp(\mathrm{i}\omega j \Delta x) \qquad\qquad u_{j-\frac{1}{2}} = \sum_\omega \hat{u}^{\text{point}}(\omega) \exp(\mathrm{i}\omega j \Delta x) \tag{B.1}$$

The summation is over all wave numbers ω that are compatible with the boundary conditions, i.e.,

$$q_{j+n} = \sum_\omega \hat{q}^{\text{avg}}(\omega) \exp(\mathrm{i}\omega (j+n) \Delta x) \equiv \sum_\omega \hat{q}^{\text{avg}}(\omega) \exp(\mathrm{i}\omega j \Delta x) = q_j \tag{B.2}$$

such that

$$\omega \Delta x = 2\pi \frac{k}{n} \qquad k = 0, \dots, n-1. \tag{B.3}$$

Since the method is linear, Fourier modes do not mix. From now on, we thus perform all calculations for just one of them and ω is treated as a parameter. It is useful to introduce the translation operator

$$\tau := \exp(\mathrm{i}\omega \Delta x) = \exp\left(2\pi \frac{k}{n} \mathrm{i}\right). \tag{B.4}$$

Indeed, for a single Fourier mode,

$$u_{j+1} = \hat{u}^{\text{avg}}(\omega) \exp(\mathrm{i}\omega (j+1) \Delta x) = \tau u_j \qquad \text{and similarly} \quad u_{j+\frac{1}{2}} = \tau u_{j-\frac{1}{2}}. \tag{B.5}$$

The dependence of τ on k shall not be made explicit in the notation.

In fact, $\tau = r^k$ that has appeared previously in Lemma A.1. The circulant matrices discussed in section A have 2×2 blocks associated with one point value and one average. With A defined in (A.1), inserting into $A\boldsymbol{u}$ a Fourier mode yields

$$(A\boldsymbol{u})_i = \sum_{j=n-i}^{n-1} A_j \hat{u} \tau^{j-n+i} + \sum_{j=0}^{n-i-1} A_j \hat{u} \tau^{i+j} \overset{\tau^n=1}{=} \tau^i \sum_{j=0}^{n-1} A_j \hat{u} \tau^j = \tau^i B_k \hat{u} \tag{B.6}$$

where $\hat{u} = \begin{pmatrix} \hat{u}^{\text{point}} \\ \hat{u}^{\text{avg}} \end{pmatrix}$. The parallel to Equation (A.5) is obvious. While the matrices B_k have been so far only used to determine the eigenvalues of A, in fact it makes sense to call B_k the *Fourier symbol* $\hat{A}$ of A that will be henceforth denoted by a hat.

Consider a generic numerical method

$$\frac{\mathrm{d}}{\mathrm{d}t}\boldsymbol{u} + A\boldsymbol{u} = 0. \tag{B.7}$$

Von Neumann stability analysis amounts to studying the eigenvalues of $\hat{A}$. Using the diagonalization $\hat{R}^{-1}\hat{\Lambda}\hat{R}$ of $\hat{A}$ in

$$\frac{\mathrm{d}}{\mathrm{d}t}\hat{R}\hat{u} + \hat{\Lambda}\hat{R}\hat{u} = 0 \tag{B.8}$$

and calling $\hat{U} := \hat{R}\hat{u}$, each component $\hat{U}_\ell$ of $\hat{U}$ fulfills the ODE

$$\frac{\mathrm{d}}{\mathrm{d}t}\hat{U}_\ell + \lambda_\ell \hat{U}_\ell = 0 \tag{B.9}$$

solved by $\hat{U}_{\ell,0}\exp(-\lambda t)$. We have preservation of the norm of $\hat{U}_\ell$ if λ is purely imaginary. Its norm decays if λ has positive real part.

B.2. Preservation of energy

Consider now a situation in which all eigenvalues of $\hat{A}$ are purely imaginary. Then[1]

$$\hat{U}^\dagger\hat{U} = \hat{U}_0^\dagger\hat{U}_0, \tag{B.10}$$

i.e., the L^2 norm of $\hat{U}$ is preserved. The L^2 norm of $\hat{u}$ is *not* preserved, but it needs to be weighted:

$$\hat{U}^\dagger\hat{U} = \hat{u}^\dagger\hat{R}^\dagger\hat{R}\hat{u}. \tag{B.11}$$

Call $\hat{M} := \hat{R}^\dagger\hat{R}$. One observes both the symmetry $\hat{M}^\dagger = \hat{M}$ and the skew-symmetry of $\hat{M}\hat{A}$:

$$\hat{M}\hat{A} = \hat{R}^\dagger\hat{R}\hat{A}\underbrace{\hat{R}^{-1}\hat{R}}_{=\mathrm{id}} = \hat{R}^\dagger\hat{\Lambda}\hat{R} = -(\hat{R}^\dagger\hat{\Lambda}\hat{R})^\dagger = -(\hat{R}^\dagger\hat{R}\hat{A})^\dagger = -(\hat{M}\hat{A})^\dagger, \tag{B.12}$$

where we have used $\Lambda^\dagger = -\Lambda$. Thus, the Fourier symbol of the matrix M is simply $\hat{R}^\dagger\hat{R}$, with as many free parameters as the dimension of the space on which $\hat{M}$ acts, one for each free scaling parameter of the eigenvector.

Consider now $A = D$, the space discretization of central Active Flux. $\hat{D}$ reads

$$\begin{pmatrix} \frac{1}{\tau} - \tau & 3 - \frac{3}{\tau} \\ \tau - 1 & 0 \end{pmatrix} \tag{B.13}$$

and its eigenvalues are

$$\lambda_\pm^{\hat{D}} = \frac{\tau - 1}{2\tau}\left(-\tau - 1 \pm \sqrt{1 + 14\tau + \tau^2}\right). \tag{B.14}$$

They are indeed imaginary, since upon the transformation $\tau \mapsto \frac{1}{\tau}$ (complex conjugation) they map into their negative

$$\frac{\frac{1}{\tau} - 1}{2}\tau\left(-\frac{1}{\tau} - 1 \pm \sqrt{1 + 14\frac{1}{\tau} + \frac{1}{\tau^2}}\right) = -\frac{\tau - 1}{2\tau}\left(-1 - \tau \pm \sqrt{\tau^2 + 14\tau + 1}\right) = -\lambda_\pm^{\hat{D}}. \tag{B.15}$$

An ingenious choice of normalization for the eigenvectors gives rise to the following Fourier symbol of the mass matrix:

$$\hat{M} = \begin{pmatrix} \alpha & \beta \\ \beta\tau & 3\alpha + \beta(1 + \tau) \end{pmatrix}. \tag{B.16}$$

[1] The dagger denotes the Hermitian (conjugate) transpose.

Here, α and β are any Laurent polynomials in τ under the condition that the matrix remains Hermitian. This is equivalent to

$$\bar{\beta} = \beta\tau, \tag{B.17}$$

$$\bar{\alpha} = \alpha. \tag{B.18}$$

If $\beta = \sum_{\ell=-s}^{s} \beta_\ell \tau^\ell$, then condition (B.17) reads

$$\bar{\beta} = \sum_{\ell=-s}^{s} \beta_\ell \tau^{-\ell} = \sum_{\ell=-s}^{s} \beta_{-\ell} \tau^\ell = \sum_{\ell=-s+1}^{s+1} \beta_{\ell-1} \tau^\ell = \sum_{\ell=-s}^{s} \beta_\ell \tau^{\ell+1} = \beta\tau. \tag{B.19}$$

The first polynomials for $s = 0, 1, 2, \ldots$ that fulfill this are, up to scaling and linear combinations,

$$0, 1 + \frac{1}{\tau}, \tau + \frac{1}{\tau^2}, \ldots \tag{B.20}$$

Similarly, α must be symmetric upon the transformation $\tau \mapsto \frac{1}{\tau}$, i.e. the first few polynomials (up to scaling and linear combinations) are

$$1, \tau + \frac{1}{\tau}, \tau^2 + \frac{1}{\tau^2}, \ldots \tag{B.21}$$

One choice is $\beta = 0$, $\alpha = 1$, yielding matrix (3.4), another is

$$\alpha = m_p + \frac{3m_p - m_v + 2m_{vv}}{6}\left(\tau + \frac{1}{\tau}\right) \in \operatorname{span}\left(1, \tau + \frac{1}{\tau}\right), \tag{B.22}$$

$$\beta = -(3m_p - m_v)\frac{1+\tau}{2\tau} \in \operatorname{span}\left(1 + \frac{1}{\tau}\right). \tag{B.23}$$

yielding (3.6). Further choices can thus be systematically derived, for instance using

$$\alpha = m_p + y\left(\tau + \frac{1}{\tau}\right) + \frac{m_{vvv} - m_{vvp}}{3}\left(\tau^2 + \frac{1}{\tau^2}\right) \in \operatorname{span}\left(1, \tau + \frac{1}{\tau}, \tau^2 + \frac{1}{\tau^2}\right),$$

$$\beta = \frac{-3m_p + m_v}{2}\left(1 + \frac{1}{\tau}\right) + m_{vvp}\left(\tau + \frac{1}{\tau^2}\right) \in \operatorname{span}\left(1 + \frac{1}{\tau}, \tau + \frac{1}{\tau^2}\right).$$

with $y := \frac{3m_p - m_v + 2m_{vv} - 2m_{vvp}}{6}$ one obtains

$$M = \left(\begin{array}{ccccccccccccc}
 & & & & \ddots & & & & & & & & \\
\frac{m_{vvv}-m_{vvp}}{3} & m_{vvp} & y & \frac{m_v-3m_p}{2} & m_p & \frac{m_v-3m_p}{2} & y & m_{vvp} & \frac{m_{vvv}-m_{vvp}}{3} & & & & \\
 & m_{vvv} & m_{vvp} & m_{vv} & \frac{m_v-3m_p}{2} & m_v & \frac{m_v-3m_p}{2} & m_{vv} & m_{vvp} & m_{vvv} & & & \\
 & & \frac{m_{vvv}-m_{vvp}}{3} & m_{vvp} & y & \frac{m_v-3m_p}{2} & m_p & \frac{m_v-3m_p}{2} & y & m_{vvp} & \frac{m_{vvv}-m_{vvp}}{3} & & \\
 & & & m_{vvv} & m_{vvp} & m_{vv} & \frac{m_v-3m_p}{2} & m_v & \frac{m_v-3m_p}{2} & m_{vv} & m_{vvp} & m_{vvv} & \\
 & & & & & & & & \ddots & & & &
\end{array}\right)$$

References

[1] R. Abgrall. "A combination of residual distribution and the active flux formulations or a new class of schemes that can combine several writings of the same hyperbolic problem: application to the 1D Euler equations." In: *Communications on Applied Mathematics and Computation* 5.1 (2023), pp. 370–402. DOI: 10.1007/s42967-021-00175-w.

[2] R. Abgrall and W. Barsukow. "Extensions of active flux to arbitrary order of accuracy." In: *ESAIM: Mathematical Modelling and Numerical Analysis* 57.2 (2023), pp. 991–1027. DOI: 10.1051/m2an/2023004.

[3] R. Abgrall, W. Barsukow, and C. Klingenberg. "A Semi-discrete Active Flux Method for the Euler Equations on Cartesian Grids." In: *Journal of Scientific Computing* 102.2 (2025), p. 36. DOI: 10.1007/s10915-024-02749-1.

[4] R. Abgrall, J. Nordström, P. Öffner, and S. Tokareva. "Analysis of the SBP-SAT Stabilization for Finite Element Methods Part I: Linear problems." In: *Journal of Scientific Computing* 85.2 (2020), pp. 1–29. DOI: 10.1007/s10915-020-01349-z. arXiv: 1912.08108 [math.NA].

[5] R. Abgrall and W. Barsukow. "A hybrid finite element - finite volume method for conservation laws." In: *Applied Mathematics and Computation* 447 (2023). DOI: https://doi.org/10.1016/j.amc.2023.127846.

[6] Abgrall, Remi and Barsukow, Wasilij. "Extensions of Active Flux to arbitrary order of accuracy." In: *ESAIM: M2AN* 57.2 (2023), pp. 991–1027. DOI: 10.1051/m2an/2023004.

[7] W. Barsukow. "Stationarity preserving schemes for multi-dimensional linear systems." In: *Mathematics of Computation* 88 (2019), pp. 1621–1645. DOI: 10.1090/mcom/3394.

[8] W. Barsukow, P. Chandrashekar, C. Klingenberg, and L. Lechner. "A generalized Active Flux method of arbitrarily high order in two dimensions." In: *arXiv preprint arXiv:2502.05101* (2025).

[9] W. Barsukow, J. Kern, C. Klingenberg, and L. Lechner. "Analysis of the multi-dimensional semi-discrete Active Flux method using the Fourier transform." In: *Communications on Applied Mathematics and Computation* (2025), pp. 1–49.

[10] W. Barsukow, C. Klingenberg, L. Lechner, J. Nordström, S. Ortleb, and H. Ranocha. *Reproducibility repository for "Stability of the Active Flux Method in the Framework of Summation-by-Parts Operators"*. https://github.com/ranocha/2025_active_flux_sbp. 2025. DOI: 10.5281/zenodo.15861045.

[11] J. Bezanson, A. Edelman, S. Karpinski, and V. B. Shah. "Julia: A Fresh Approach to Numerical Computing." In: *SIAM Review* 59.1 (2017), pp. 65–98. DOI: 10.1137/141000671. arXiv: 1411.1607 [cs.MS].

[12] M. H. Carpenter, T. C. Fisher, E. J. Nielsen, and S. H. Frankel. "Entropy Stable Spectral Collocation Schemes for the Navier-Stokes Equations: Discontinuous Interfaces." In: *SIAM Journal on Scientific Computing* 36.5 (2014), B835–B867. DOI: 10.1137/130932193.

[13] M. H. Carpenter, D. Gottlieb, and S. Abarbanel. "Time-Stable Boundary Conditions for Finite-Difference Schemes Solving Hyperbolic Systems: Methodology and Application to High-Order Compact Schemes." In: *Journal of Computational Physics* 111.2 (1994), pp. 220–236. DOI: 10.1006/jcph.1994.1057.

[14] J. Chan. "On discretely entropy conservative and entropy stable discontinuous Galerkin methods." In: *Journal of Computational Physics* 362 (2018), pp. 346–374. DOI: 10.1016/j.jcp.2018.02.033.

[15] S. Danisch and J. Krumbiegel. "Makie.jl: Flexible high-performance data visualization for Julia." In: *Journal of Open Source Software* 6.65 (2021), p. 3349. DOI: 10.21105/joss.03349.

[16] P. J. Davis. *Circulant Matrices*. New York: Wiley Interscience, 1979.

[17] L. Dovgilovich and I. Sofronov. "High-accuracy finite-difference schemes for solving elastodynamic problems in curvilinear coordinates within multiblock approach." In: *Applied Numerical Mathematics* 93 (2015), pp. 176–194. DOI: 10.1016/j.apnum.2014.06.005.

[18] T. Eymann and P. Roe. "Active flux schemes for systems." In: *20th AIAA computational fluid dynamics conference* AIAA 2011-3840 (2011). DOI: 10.2514/6.2011-3840.

[19] T. A. Eymann and P. L. Roe. "Active Flux Schemes." In: *49th AIAA Aerospace Sciences Meeting including the New Horizons Forum and Aerospace Exposition* (2011). DOI: 10.2514/6.2011-382.

[20] T. A. Eymann and P. L. Roe. "Multidimensional Active Flux Schemes." In: *21st AIAA Computational Fluid Dynamics Conference* (2013). DOI: 10.2514/6.2013-2940.

[21] D. C. D. R. Fernández, J. E. Hicken, and D. W. Zingg. "Review of summation-by-parts operators with simultaneous approximation terms for the numerical solution of partial differential equations." In: *Computers & Fluids* 95 (2014), pp. 171–196. DOI: 10.1016/j.compfluid.2014.02.016.

[22] G. J. Gassner. "A Skew-Symmetric Discontinuous Galerkin Spectral Element Discretization and Its Relation to SBP-SAT Finite Difference Methods." In: *SIAM Journal on Scientific Computing* 35.3 (2013), A1233–A1253. DOI: 10.1137/120890144.

[23] J. Glaubitz, S.-C. Klein, J. Nordström, and P. Öffner. "Multi-dimensional summation-by-parts operators for general function spaces: Theory and construction." In: *Journal of Computational Physics* 491 (2023). DOI: 10.1016/j.jcp.2023.112370.

[24] J. Glaubitz, S.-C. Klein, J. Nordström, and P. Öffner. "Summation-by-parts operators for general function spaces: The second derivative." In: *Journal of Computational Physics* 504 (2024). DOI: 10.1016/j.jcp.2024.112889.

[25] J. Glaubitz, J. Nordström, and P. Öffner. "Summation-by-Parts Operators for General Function Spaces." In: *SIAM Journal on Numerical Analysis* 61.2 (2023), pp. 733–754. DOI: 10.1137/22M1470141.

[26] J. Glaubitz, J. Nordström, and P. Öffner. "Energy-Stable Global Radial Basis Function Methods on Summation-By-Parts Form." In: *Journal of Scientific Computing* 98.1 (2024). DOI: 10.1007/s10915-023-02427-8.

[27] E. Hairer, C. Lubich, and G. Wanner. *Geometric Numerical Integration: Structure-Preserving Algorithms for Ordinary Differential Equations*. Vol. 31. Springer Series in Computational Mathematics. Berlin Heidelberg: Springer-Verlag, 2006. DOI: 10.1007/3-540-30666-8.

[28] J. Hicken, G. Yan, and S. Kaur. *Constructing stable, high-order finite-difference operators on point clouds over complex geometries*. Sept. 2024. arXiv: 2409.00809 [math.NA].

[29] J. E. Hicken. "Entropy-stable, high-order summation-by-parts discretizations without interface penalties." In: *Journal of Scientific Computing* 82.2 (2020), p. 50. DOI: 10.1007/s10915-020-01154-8.

[30] J. E. Hicken, D. C. D. R. Fernández, and D. W. Zingg. "Multidimensional Summation-By-Parts Operators: General Theory and Application to Simplex Elements." In: *SIAM Journal on Scientific Computing* 38.4 (2016), A1935–A1958. DOI: 10.1137/15M1038360.

[31] H. T. Huynh. "A Flux Reconstruction Approach to High-Order Schemes Including Discontinuous Galerkin Methods." In: *18th AIAA Computational Fluid Dynamics Conference*. American Institute of Aeronautics and Astronautics. 2007. DOI: 10.2514/6.2007-4079.

[32] D. I. Ketcheson. "Relaxation Runge-Kutta Methods: Conservation and Stability for Inner-Product Norms." In: *SIAM Journal on Numerical Analysis* 57.6 (2019), pp. 2850–2870. DOI: 10.1137/19M1263662. arXiv: 1905.09847 [math.NA].

[33] H.-O. Kreiss and G. Scherer. "Finite Element and Finite Difference Methods for Hyperbolic Partial Differential Equations." In: *Mathematical Aspects of Finite Elements in Partial Differential Equations*. Ed. by C. de Boor. New York: Academic Press, 1974, pp. 195–212.

[34] B. V. Leer. "Towards the ultimate conservative difference scheme. IV. A new approach to numerical convection." In: *Journal of Computational Physics* 23.3 (1977), pp. 276–299. DOI: 10.1016/0021-9991(77)90095-X.

[35] C. Lozano. "Entropy Production by Explicit Runge-Kutta Schemes." In: *Journal of Scientific Computing* 76.1 (2018), pp. 521–565. DOI: 10.1007/s10915-017-0627-0.

[36] L. Lundgren and K. Mattsson. "An efficient finite difference method for the shallow water equations." In: *Journal of Computational Physics* 422 (2020), p. 109784. DOI: 10.1016/j.jcp.2020.109784.

[37] K. Mattsson. "Diagonal-norm upwind SBP operators." In: *Journal of Computational Physics* 335 (2017), pp. 283–310. DOI: 10.1016/j.jcp.2017.01.042.

[38] K. Mattsson, M. Svärd, M. Carpenter, and J. Nordström. "High-order accurate computations for unsteady aerodynamics." In: *Computers & Fluids* 36.3 (2007), pp. 636–649. DOI: 10.1016/j.compfluid.2006.02.004.

[39] J. Nordström and M. Björck. "Finite volume approximations and strict stability for hyperbolic problems." In: *Applied Numerical Mathematics* 38.3 (2001), pp. 237–255. DOI: 10.1016/S0168-9274(01)00027-7.

[40] J. Nordström, K. Forsberg, C. Adamsson, and P. Eliasson. "Finite volume methods, unstructured meshes and strict stability for hyperbolic problems." In: *Applied Numerical Mathematics* 45.4 (2003), pp. 453–473. DOI: 10.1016/S0168-9274(02)00239-8.

[41] P. Olsson. "Summation by parts, projections, and stability. I." In: *Mathematics of Computation* 64.211 (1995), pp. 1035–1065. DOI: 10.2307/2153512.

[42] P. Olsson. "Summation by parts, projections, and stability. II." In: *Mathematics of Computation* 64.212 (1995), pp. 1473–1493. DOI: 10.2307/2153366.

[43] S. Ortleb. "A kinetic energy preserving DG scheme based on Gauss-Legendre points." In: *Journal of Scientifc Computing* 71 (2017), pp. 1135–1168. DOI: 10.1007/s10915-016-0334-2.

[44] S. Ortleb. "On the Stability of IMEX Upwind gSBP Schemes for 1D Linear Advection-Diffusion Equations." In: *Communications on Applied Mathematics and Computation* (2023). DOI: 10.1007/s42967-023-00296-4.

[45] H. Ranocha. "On Strong Stability of Explicit Runge-Kutta Methods for Nonlinear Semibounded Operators." In: *IMA Journal of Numerical Analysis* 41.1 (Jan. 2021), pp. 654–682. DOI: 10.1093/imanum/drz070. arXiv: 1811.11601 [math.NA].

[46] H. Ranocha, L. Dalcin, M. Parsani, and D. I. Ketcheson. "Optimized Runge-Kutta Methods with Automatic Step Size Control for Compressible Computational Fluid Dynamics." In: *Communications on Applied Mathematics and Computation* 4 (Nov. 2021), pp. 1191–1228. DOI: 10.1007/s42967-021-00159-w. arXiv: 2104.06836 [math.NA].

[47] H. Ranocha and D. I. Ketcheson. "Energy Stability of Explicit Runge-Kutta Methods for Nonautonomous or Nonlinear Problems." In: *SIAM Journal on Numerical Analysis* 58.6 (Nov. 2020), pp. 3382–3405. DOI: 10.1137/19M1290346. arXiv: 1909.13215 [math.NA].

[48] H. Ranocha, L. Lóczi, and D. I. Ketcheson. "General Relaxation Methods for Initial-Value Problems with Application to Multistep Schemes." In: *Numerische Mathematik* 146 (Oct. 2020), pp. 875–906. DOI: 10.1007/s00211-020-01158-4. arXiv: 2003.03012 [math.NA].

[49] H. Ranocha, D. Mitsotakis, and D. I. Ketcheson. "A Broad Class of Conservative Numerical Methods for Dispersive Wave Equations." In: *Communications in Computational Physics* 29 (4 2021), pp. 979–1029. DOI: 10.4208/cicp.OA-2020-0119.

[50] H. Ranocha and P. Öffner. "L_2 Stability of Explicit Runge-Kutta Schemes." In: *Journal of Scientific Computing* 75.2 (May 2018), pp. 1040–1056. DOI: 10.1007/s10915-017-0595-4.

[51] H. Ranocha, P. Öffner, and T. Sonar. "Summation-by-parts operators for correction procedure via reconstruction." In: *Journal of Computational Physics* 311 (Apr. 2016), pp. 299–328. DOI: 10.1016/j.jcp.2016.02.009. arXiv: 1511.02052 [math.NA].

[52] H. Ranocha, M. Sayyari, L. Dalcin, M. Parsani, and D. I. Ketcheson. "Relaxation Runge-Kutta Methods: Fully-Discrete Explicit Entropy-Stable Schemes for the Compressible Euler and Navier-Stokes Equations." In: *SIAM Journal on Scientific Computing* 42.2 (Mar. 2020), A612–A638. DOI: 10.1137/19M1263480. arXiv: 1905.09129 [math.NA].

[53] H. Ranocha, A. R. Winters, M. Schlottke-Lakemper, P. Öffner, J. Glaubitz, and G. J. Gassner. "On the robustness of high-order upwind summation-by-parts methods for nonlinear conservation laws." In: *Journal of Computational Physics* 520 (2025), p. 113471. DOI: https://doi.org/10.1016/j.jcp.2024.113471.

[54] P. Roe. "Designing CFD methods for bandwidth—A physical approach." In: *Computers & Fluids* 214 (2021), p. 104774.

[55] V. Stiernström, L. Lundgren, M. Nazarov, and K. Mattsson. "A residual-based artificial viscosity finite difference method for scalar conservation laws." In: *Journal of Computational Physics* 430 (2021), p. 110100. DOI: https://doi.org/10.1016/j.jcp.2020.110100.

[56] B. Strand. "Summation by Parts for Finite Difference Approximations for d/dx." In: *Journal of Computational Physics* 110.1 (1994), pp. 47–67. DOI: 10.1006/jcph.1994.1005.

[57] Z. Sun and C.-W. Shu. "Stability of the fourth order Runge-Kutta method for time-dependent partial differential equations." In: *Annals of Mathematical Sciences and Applications* 2.2 (2017), pp. 255–284. DOI: 10.4310/AMSA.2017.v2.n2.a3.

[58] Z. Sun and C.-W. Shu. "Strong Stability of Explicit Runge-Kutta Time Discretizations." In: *SIAM Journal on Numerical Analysis* 57.3 (2019), pp. 1158–1182. DOI: 10.1137/18M122892X. arXiv: 1811.10680 [math.NA].

[59] M. Svärd. "On Coordinate Transformations for Summation-by-Parts Operators." In: *Journal of Scientific Computing* 20.1 (2004), pp. 29–42. DOI: 10.1023/A:1025881528802.

[60] M. Svärd, K. Mattsson, and J. Nordström. "Steady-state computations using summation-by-parts operators." In: *Journal of Scientific Computing* 24 (2005), pp. 79–95. DOI: 10.1007/s10915-004-4788-2.

[61] M. Svärd and J. Nordström. "On the convergence rates of energy-stable finite-difference schemes." In: *Journal of Computational Physics* 397 (2019), p. 108819. DOI: 10.1016/j.jcp.2019.07.018.

[62] M. Svärd and J. Nordström. "Review of summation-by-parts schemes for initial-boundary-value problems." In: *Journal of Computational Physics* 268 (2014), pp. 17–38. DOI: 10.1016/j.jcp.2014.02.031.

[63] E. Tadmor. "From Semidiscrete to Fully Discrete: Stability of Runge-Kutta Schemes by the Energy Method II." In: *Collected Lectures on the Preservation of Stability under Discretization*. Ed. by D. J. Estep and S. Tavener. Vol. 109. Proceedings in Applied Mathematics. Philadelphia: Society for Industrial and Applied Mathematics, 2002, pp. 25–49.

[64] G. E. Trapp. "Inverses of circulant matrices and block circulant matrices." In: *Kyungpook Mathematical Journal* 13.1 (1973), pp. 11–20.

[65] P. E. Vincent, P. Castonguay, and A. Jameson. "A New Class of High-Order Energy Stable Flux Reconstruction Schemes." In: *Journal of Scientific Computing* 47.1 (2011), pp. 50–72. DOI: 10.1007/s10915-010-9420-z.

Conflict of interest

Not applicable.